Supporting Information.

Legends to Figures S1-S5

Figure S1. pH-dependence of cytochrome *c* oxidase activity of N139L mutant and wild type oxidase from *R. sphaeroides*.

Cytochrome oxidase activity was measured at different pH values following oxygen consumption with a Clark-type electrode as described in "Materials and Methods". *Filled squares*, wild type enzyme. *Open squares*, N139L mutant. *Open circles*, the data for N139L have been normalized to the activity of the wild type enzyme (dividing by the average inhibition value of 7%) in order to facilitate visual comparison of the pH dependencies. See "Materials and Methods" for the conditions.

Figure S2. Proton-pumping measurements with N139L mutant (A) and wild type (B) cytochrome c oxidase from *R. sphaeroides*.

For the conditions, see "Materials and Methods". The arrows labeled as H^+ indicate acidification induced by addition of 10 µl of 1 mM HCl (10 nmol) to the cell. O_2 additions, 2.5 nmol. In case of the curves 2, 30 µM carbonyl cyanide *m*-chlorophenyl hydrazone (CCCP), the uncoupler, was also present.

Figure S3. Deconvolution of the kinetics of heme *a* reoxidation in the wild type oxidase.

Fitting of the heme *a* reoxidation kinetics has been performed by two different protocols, as described below. 36 individual traces have been averaged to provide for good signal-to-noise ratio. A single-exponential approximation gave very poor results (not shown). **Figure S3,A** shows 2 exponential deconvolution made as in our previous work (*1*). Although the fit is reasonably good, there is an obvious shortcoming of such deconvolution: - neither the time

constants nor the relative magnitudes of the two components match the characteristics of the two phases of $\Delta\psi$ generation coupled to the reoxidation of heme a (cf. ref. 1 and **Table 2**). Therefore, an alternative fitting procedure has been used (**Figure S3, B**), assuming that the phases of heme a reoxidation, monitored optically, are related to the proton transfer phases in the kinetics of $\Delta\psi$ generation measured electrometrically (cf. **Table 2**). In case of the wild type oxidase, the signal-to-noise ratio is very much better for the electrometric curves as compared to the absorption traces (e.g., cf. **Figure 5**) . Therefore, the fitting of the absorption traces was performed by setting fixed lifetimes for the two major components of heme a reoxidation, choosing the τ values from the deconvolution of the electrometric curves ($\tau_1 \sim 0.4$ ms and $\tau_2 \sim 1.6$ ms, **Table 2**). With these τ values, a very good fit can be obtained for the absorption trace, provided a minor third slow component with $\tau > 8$ ms and contribution of 5-15% is included. An example of such fitting is shown in **Figure S3,B** and the results are given in **Table 1.** A plot of the residuals and other fitting parameters in **Figure S3,B** are slightly but noticeably better than for the 2 exponential fit in **Figure S3,A,** but, what is more important, the amplitude ratio of the 0.4 ms and 1.6 ms phases of heme a reoxidation found with the new protocol, becomes close to the amplitude ratio of the 0.4 ms and 1.6 ms resolved for the electrogenic phases. The minor component with τ of 8-10 ms is too slow for the wild type oxidase turnover and may correspond to a small fraction of damaged enzyme (cf. the 5-10% of the slowly oxidizing wild type enzyme in **Figure 1A**).

Figure S4. Comparison of the electrogenic responses coupled to the photoinduced F $\rightarrow$ O transition in the wild type, N139D and N139L mutant forms of cytochrome oxidase from *R. sphaeroides*.

Experiments with collodion film-adhered liposomes with COX have been carried out in the buffer containing 5 mM Tris-acetate, pH 8, with 40 μM RuBpy and 10 mM aniline as the photoreducing system. 2 mM H_2O_2 was added to convert COX to the ferryl-oxo state prior to the

flash. The traces have been normalized by the magnitude of the microsecond KCN-insensitive part of the response.

Figure S5. Resolution of the cyanide-sensitive slow phase of membrane potential generation coupled to the photoinduced F→O transition in N139L mutant oxidase.

As shown in **Figure S4,** the rapid microsecond phase of $\Delta\psi$ generation in the N139L mutant oxidase, is not followed by any significant additional electrogenic phase(s) in the conventional ~10 ms time wndow, in which the electrogenic protonic phases of the wild type enzyme and N139D mutant are fully developed. However, it is well known that with the electrometric technique, low-amplitude slow phases of membrane potential generation (tens of milliseconds or slower) can be masked by passive discharge of $\Delta\psi$ (e.g., (*2, 3*)). The passive discharge is a multiphasic process that may take up to several seconds for completion. **Figure S5** compares the photoelectric responses of the N139L mutant at a slower sweep in the absence (trace *a*) and in the presence of cyanide (trace *b*). It can be seen that the addition of KCN to N139L mutant oxidase enhances markedly $\Delta\psi$ decay that follows the microsecond phase of $\Delta\psi$ generation (cf. traces *a* and *b* in **Figure S5**). Subtracting trace *b* taken in the presence of KCN from trace *a* taken in the absence of KCN allows to elicit a slow KCN-sensitive phase of membrane potential generation (trace *c*) inherent in the electrogenic response of the N139L oxidase. The phase corresponds to low-magnitude vectorial charge movement, most probably H^+ transfer, linked to the KCN-sensitive electron transfer from heme *a* to the binuclear center (see the text and **Figure 10**). Trace *d* simulates protonic phase of $\Delta\psi$ generation that should be observed if E286, after donating proton to the binuclear site (cf. **Figures 8-10**), were reprotonated from the N-phase with k = 2 s^{-1}, corresponding to the rate of the **F→O** transition during the oxidation of the fully reduced N139L oxidase by oxygen (cf. **Figures 2, 8B, 9** and relevant text in Discussion).

Conditions: (*a*) as in **Figure S4;** (*b*) after addition of 0.5 mM KCN. In (*b*), 200 µM

ferricyanide was also present to prevent spontaneous reduction of heme a in the cyanide-inhibited oxidase by endogenous electron donors.

REFERENCES

1.   Siletsky, S. A., Pawate, A. S., Weiss, K., Gennis, R. B., and Konstantinov, A. A. (2004) Transmembrane charge separation during the ferryl-oxo $\rightarrow$ oxidized transition in a non-pumping mutant of cytochrome c oxidase. *J. Biol. Chem 279*, 52558-52565.

2.   Gopta, O. A., Feniouk, B. A., Junge, W., and Mulkidjanian, A. Y. (1998) The cytochrome bc_1 complex of *Rhodobacter capsulatus:* Ubiquinol oxidation in a dimeric Q-cycle?, *FEBS Lett 431*, 291-296.

3.   Mamedov, M. D., Tyunyatkina, A. A., Siletsky, S. A., and Semenov, A. Y. (2006) Voltage changes involving photosystem II quinone-iron complex turnover. *Eur Biophys J 35*, 647-654.
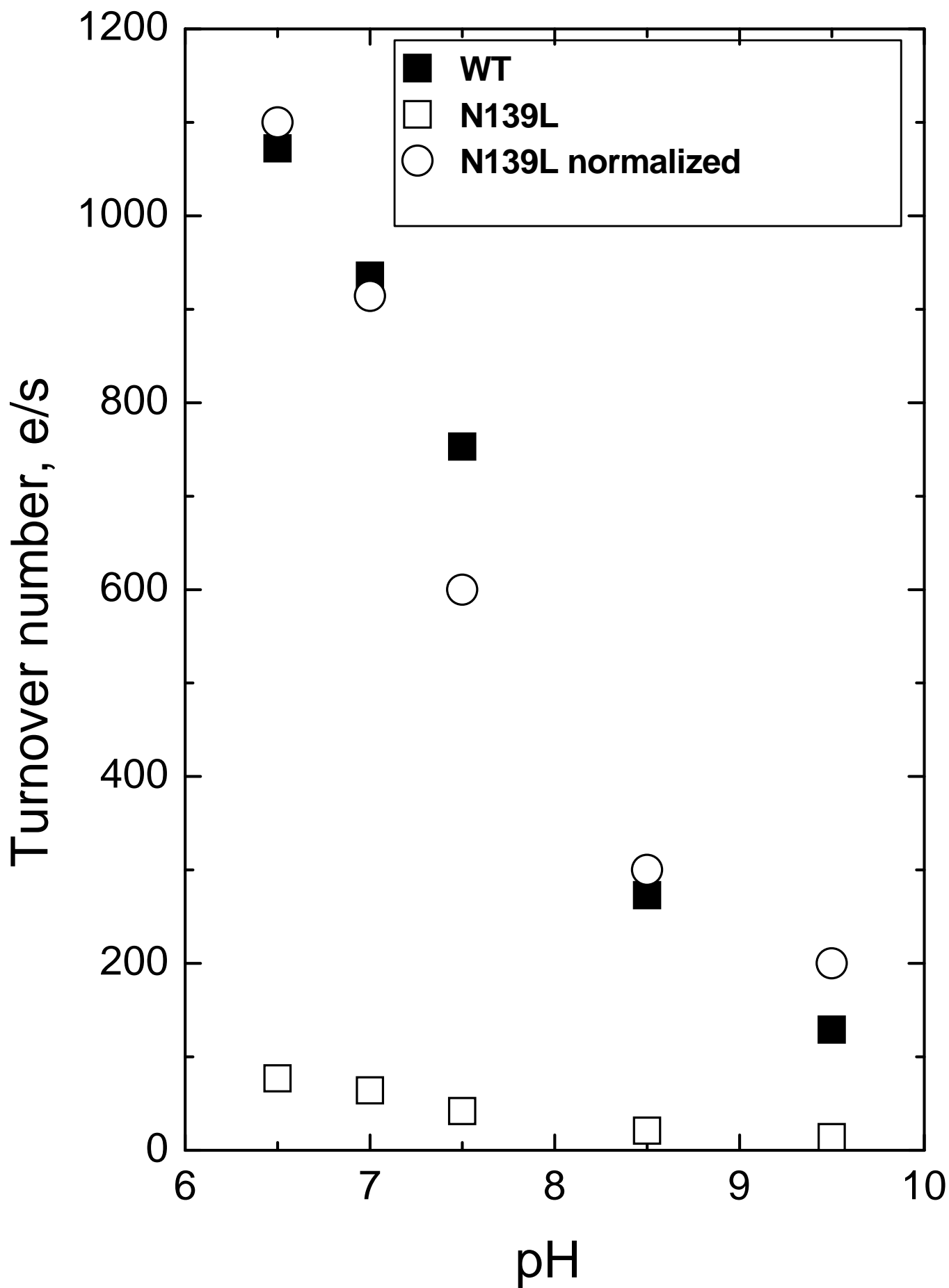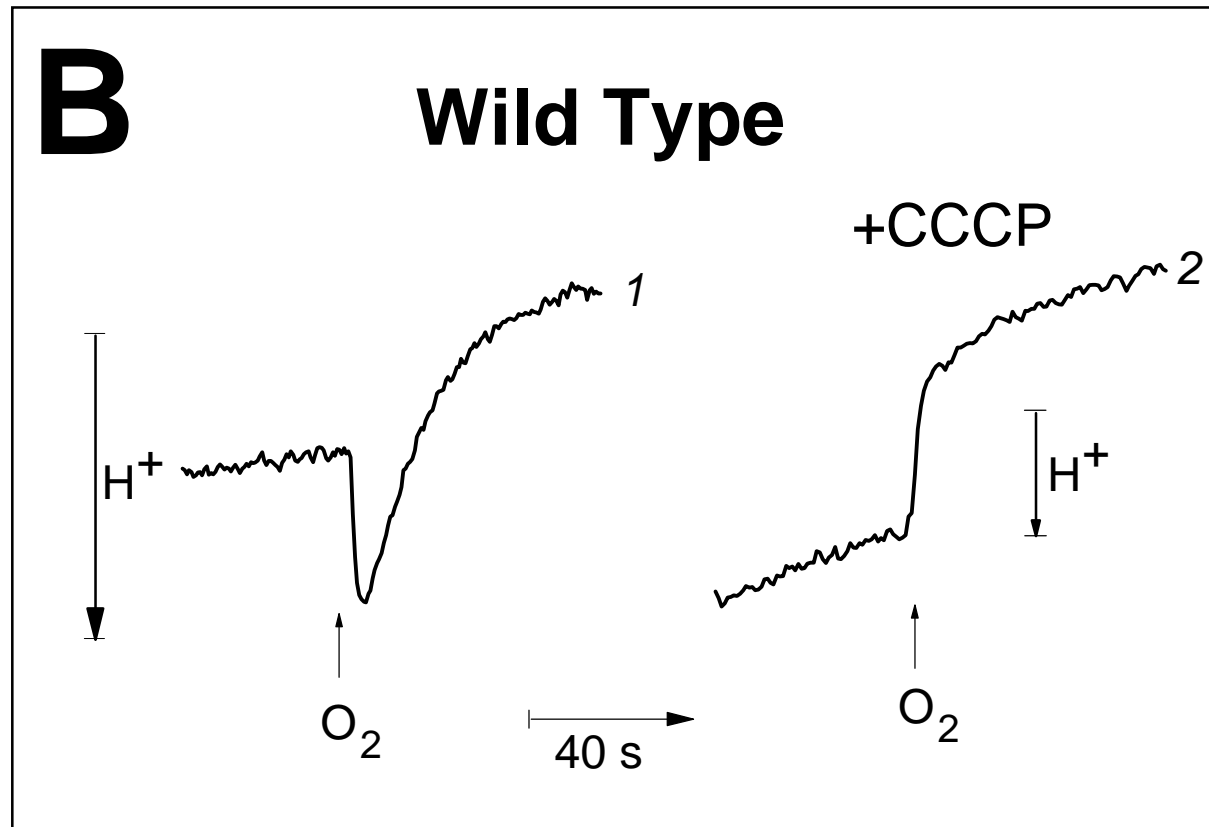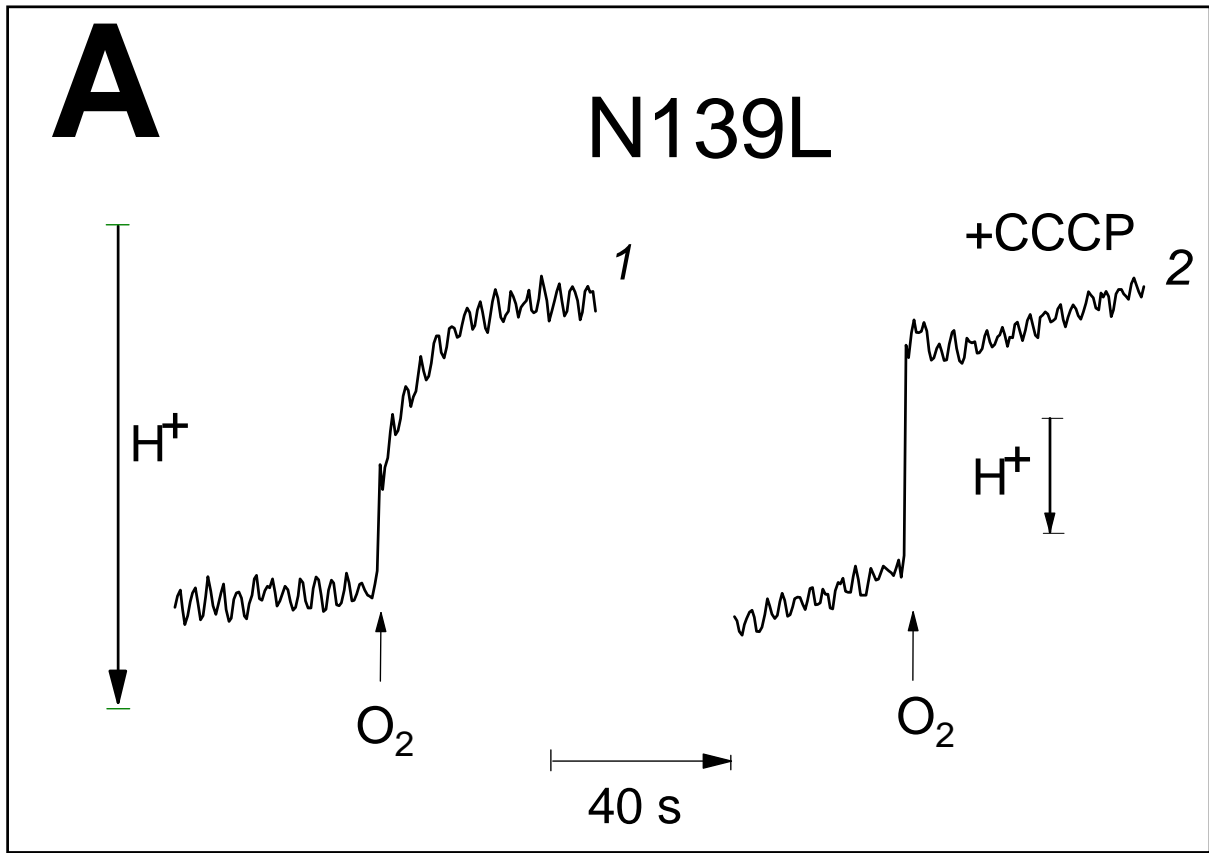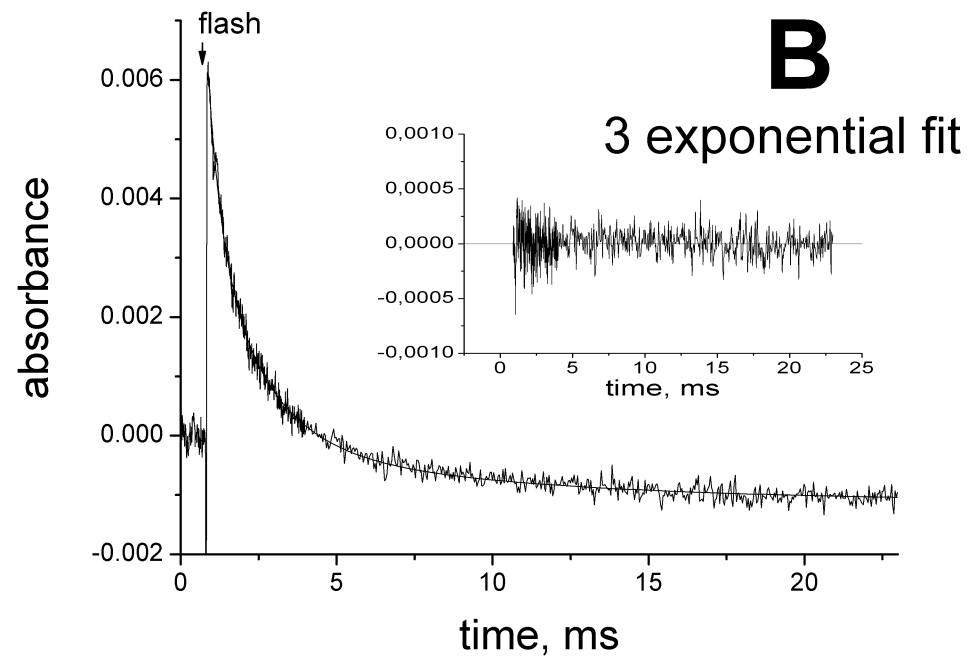
Figure S1

Figure S2

A   N139L

+CCCP

H$^+$

O$_2$

40 s

B   Wild Type

+CCCP

H$^+$

O$_2$

40 s

Figure S3

A — 2 exponential fit
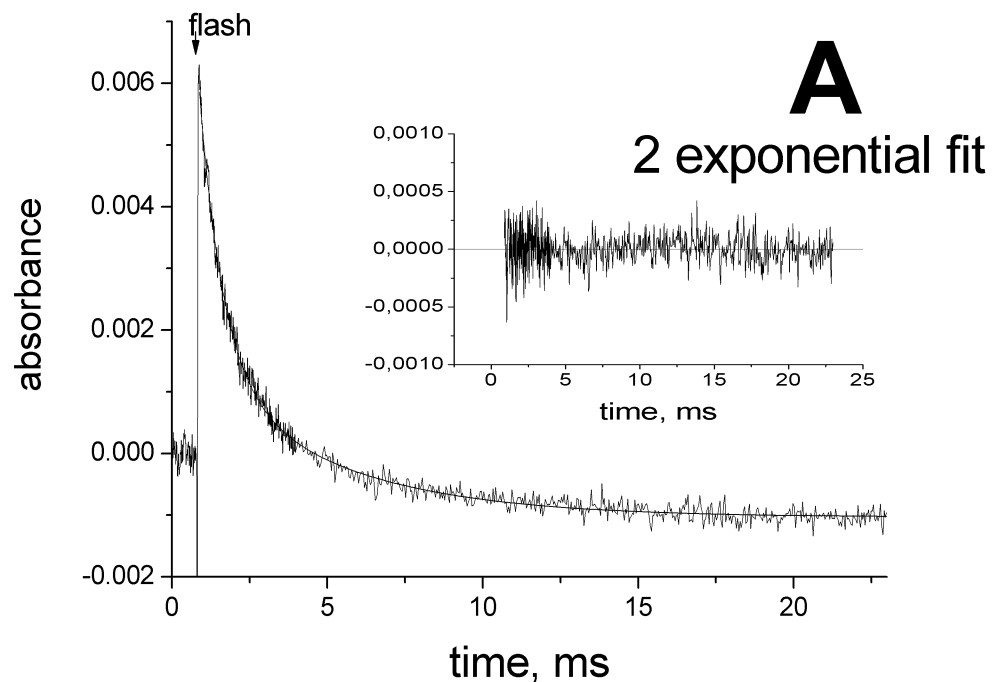
Chi^2/DoF = 1.9974E -8
R^2 = 0.99234
A_1 = 0.00457 ± 0.00008

τ_1 = 0.76675 ±0.02003
A_2 = 0.00232 ± 0.00008

τ_2 = 4.37135 ±0.20021

B — 3 exponential fit

Chi^2/DoF = 1.991E-8
R^2 = 0.99236
A_1 = 0.00235 ±0.00006
τ_1 = 0.4
A_2 = 0.00375 ± 0.00006
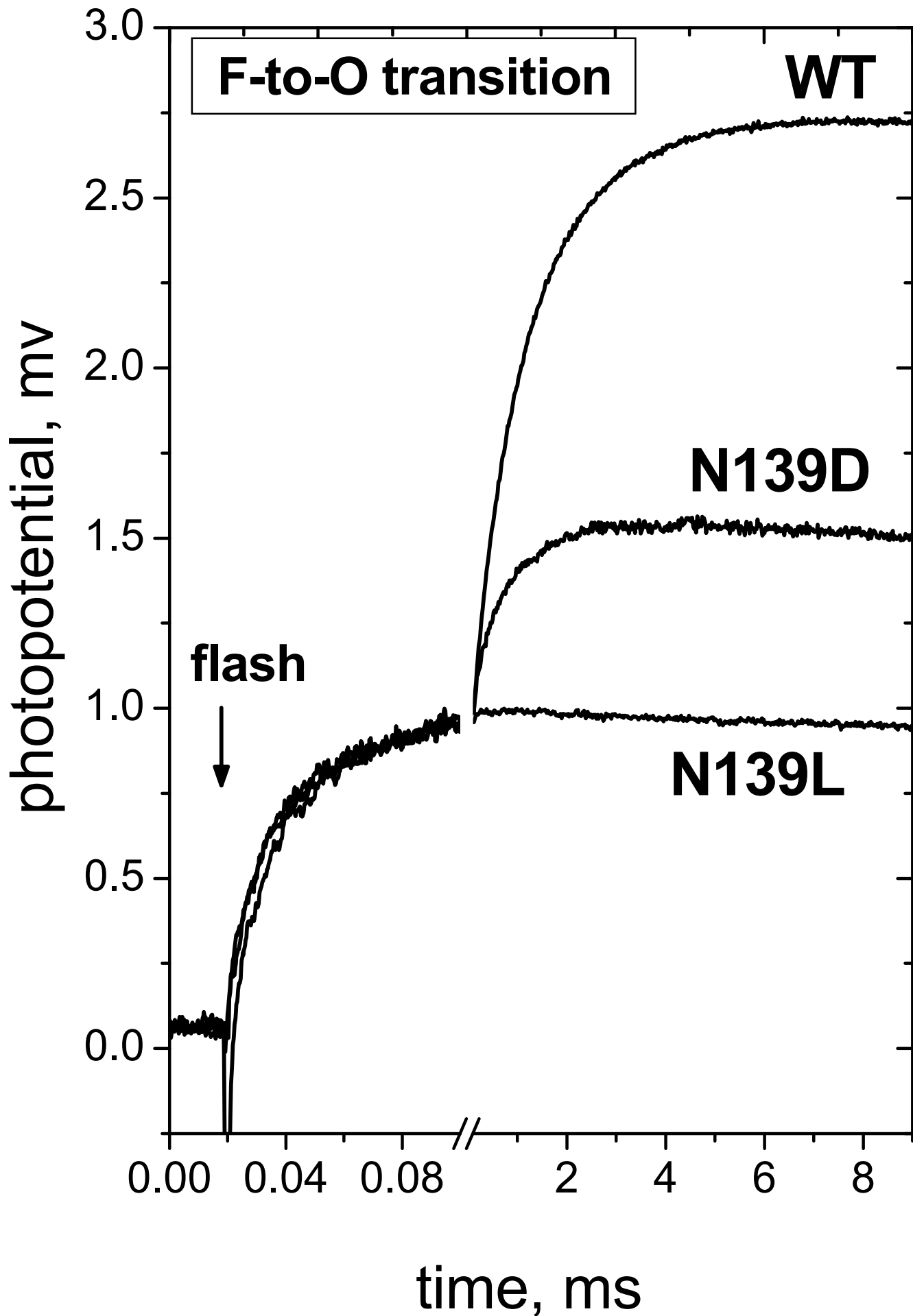τ_2 = 1.6
A_3 = 0.00109 ± 0.00004
τ_3 = 8

Figure S4

Figure S5

F-to-O transition   N139L

flash

d = c + phase with τ~0.5 s

a

b

c

d

photopotenital, mv

time, ms